Proceedings of ASME Turbo Expo 2011
GT2011
June 6-10, 2011, Vancouver, British Columbia, Canada

GT2011-45504

TIP RUNNING CLEARANCES EFFECTS ON TIP VORTICES INDUCED AXIAL COMPRESSOR ROTOR FLUTTER

Dr Caetano Peng
Rolls-Royce Plc.
Fans SCU
Moor Lane Building ML-44 D2
PO Box 31 Derby
DE24 8BJ England
United Kingdom

ABSTRACT

The present study aimed at investigating numerically the effects of large blade tip running clearances on flutter stability of axial core multi-stage compressor rotor. During this study, the influences of aerodynamic boundary conditions, variable stator vane incidence and tip running clearances of upstream and downstream rotors on aerodynamic compressor flow and rotor flutter stability are thoroughly investigated. The simulations were carried out using an in-house 3-D aeroelasticity code. The steady-state-solution computations are performed on single-blade-passage-one-bladerow, stage-blocks and whole compressor models. These analyses included rotor blade models with nominal tip running clearances and artificially large tip clearances. Moreover, the effects of the variable stator vane incidences are assessed by performing steady-state-solution computations for nominal vane schedules and extreme vane malschedule. The first four flap and torsion vibration modes from finite element analyses are included in the unsteady flow computations and assessed for flutter stability.

The results from the numerical investigations showed that the compressors with large rotor tip running clearances are susceptible to rotor tip flow induced flutter instability. The aerodynamic losses on the rotor with large tip clearances increase with other rotors having also large tip gaps. For the aerodynamic boundary conditions considered here, the simulations predicted flutter instability for the first flap vibration mode. The flutter instability predicted on the rotors with large tip clearances is driven by oscillating tip vortices on blade suction surface close to the blade tip leading edge. The flow in the rotor tip gap is mostly stalled and tip vortices oscillations are close to blade tip leading edge. The strength of these oscillating vortices appears to increase with increase in variable stator vane malschedule or negative incidence. Small changes in aerodynamic conditions can offset these instabilities. These studies indicate that the main ingredients for the occurrence of these phenomena are likely to be excessively large rotor tip running clearances combined with significant changes in flow incidence.

NOMENCLATURE

CFD	Computational Fluid Dynamics
FE	Finite Element
BC	Boundary conditions
HCF	High Cycle Fatigue
FFT	Fast Fourier Transform
EO	Engine order
LE	Leading edge
TE	Trailing edge
ζ	Damping parameter
Uvel	Axial flow velocity
f	Modal frequency
ND	Nodal diameter (inter-blade-phase angle)
NSN	Non-synchronous vibration
VSV	Variable stator vanes
Logdec	Logarithmic decay
IPC	Intermediate pressure compressor

1. INTRODUCTION

Compressor rotor flutter phenomena are aerodynamic self-excited instabilities that result from unbalanced exchanges of energy between aerodynamic gas flow and the structural rotor blades in which the flow tends to provide more energy that can be absorbed by the rotor blades. Their occurrence can be expressed as rotor negative damping. The catastrophic consequences of these phenomena associated with rapid high cycle fatigue (HCF) failure of rotor blades are well known. These phenomena have been studied both experimentally and analytically for several decades. Stall and choke flutter phenomena are reasonably well understood and they can be predicted to some extent using the state-of-the-art Computation Fluid Dynamics (CFD) aeroelasticity tools. However, flutter induced by the effects of relatively large blade tip running clearances has not been widely investigated both experimentally and numerically because real engine or rig tests are very expensive and the current numerical tools experience some difficulties in running with relatively large blade tip leakage.

There would appear that very few papers and literature have been published on the effects of tip leakage on flutter of rotor blades. The studies on the influence of tip leakage flow on aerodynamic damping were done mostly for linear cascade of flat plates in a 2-D flapping oscillation. One of recent experimental and numerical studies on a linear turbine cascade by Huang, He and Bell [1] showed that blade flutter stability is significantly reduced with increase in tip clearances. Their experimental results indicated that small tip clearance (1-2% blade span) flow tends to provide some stabilizing effect on the blade suction surface near the tip. For large tip clearance (~4%span), a destabilizing effect was observed around 80% chord on the suction surface. This destabilising effect is associated with a well-developed tip clearance vortex. Yang and He [2] have carried out similar type of experimental studies to [1] on a linear compressor cascade. They showed that the blades aeroelastic stability decreases with increase in the tip gap. They found that the aerodynamic damping of the least stable nodal diameter was reduced by 27% as the tip clearance was increased from 0 to 2% blade span.

Kielb et al. [3, 4] investigated a similar phenomenon to tip gap flow induced flutter that they termed non-synchronous vibration (NSV). The NSV is described as an aerodynamic instability phenomenon that results from the interactions between vortex shedding and blade vibrations. Unlike flutter, this phenomenon manifests itself when the frequency of aerodynamic instability is close to the blade natural frequency. They observed that the measured NSV vibrations are frequency and phase locked like in flutter phenomenon. However, the NSV tends to occur even if the reduced frequency values (i.e. flutter parameters) are well within the conventional flutter stable regions. Mailach et al. [5, 6] carried out interesting experimental studies on a four-stage low speed research compressor and a linear cascade to assess the effects of tip flow instability. They concluded that the tip flow instability results from a vortex interaction effect that generates rotating stall. This instability tends to occur near the stall region and it is associated with large tip clearances (i.e. gap >2% of tip chord). Recently, Thomassin and Vo [7] studied the tip flow instability effect in high-speed high pressure compressors (HPC) and proposed a physical mechanism to explain the NSV phenomenon. The NSV mechanism is modelled as the blade tip trailing edge impinging jet like flow and relies on the acoustic feedback in the jet potential. This model appears to predict the critical tip speed at which NSV can occur.

Here, the present study aimed at investigating numerically the effects of large blade tip running clearances on flutter stability of axial core multi-stage compressor rotor. During this study, the influences of aerodynamic boundary conditions, variable stator vane incidence and tip running clearances of upstream and downstream rotors on aerodynamic compressor flow and rotor flutter stability are thoroughly investigated. The phenomenon studied herein may have some features similar to those described for NSV. However here, it is treated as flutter phenomenon controlled by the effects of tip clearance. These flutter simulations are performed using an in-house aeroelasticity suite.

2. ANALYSIS METHODOLOGY

The study presented here is conducted on an eight-stage intermediate pressure compressor with seventeen bladerows. Relatively large blade tip clearances are arbitrarily chosen and applied to the whole compressor to assess the effects of tip running gap size on flutter stability of front rotors of the compressor. The first four vibration modes from FE analyses are assessed for flutter stability. The aeroelasticity simulations are performed using an in-house aeroelasticity suite named AU3D. This CFD based tool allows computations of both steady-state-solution and unsteady flow computations on small and large-scale models. Aerodynamic boundary conditions and speed are also arbitrarily selected.

FE computations are performed first to obtain the frequencies and modeshapes of vibration modes of interest. Then CFD steady-state-solution simulations are performed on single-blade-passage-one-bladerow, single-blade-passage-block-stages and single-blade-passage-whole-compressor models. The solutions from steady-state-flow computations are then used as starting solutions in the unsteady-flow simulations. The unsteady-flow flutter computations (with blade motion) are performed on full-annulus-single-bladerow models. Both steady-state-solution and unsteady-flow simulations included the effects of nominal (design) and large blade tip running clearances. Moreover, the effects of incidence are investigated by conducting compressor analyses with nominal variable vane schedule (VSV) and extreme vane malschedule. Note that the nominal VSV schedule is a non-optimised schedule. Then, the results expressed in terms of aerodynamic damping parameter are compared to evaluate the effects of tip flow and incidence.

2.1 AU3D Suite

The basic aeroelasticity suite comprises of AU3D CFD based aeroelasticity code, SC03 FE analysis tool and FORSE multi-harmonic balance forced response program. The FORSE is not used in the computations described herein. SC03 FE code is used to compute the natural vibration frequencies and modeshapes of vibration modes that are then interpolated onto CFD grids for the unsteady flow flutter simulations. The AU3D main solver is 3-D Reynolds averaged Navier-Stokes equations based code that uses a time-marching scheme. The description of AU3D code can be found in the references [8, 9, 10 and 11]. The aeroelasticity suite has been used over a wide range of applications. This system is illustrated in Fig.1.

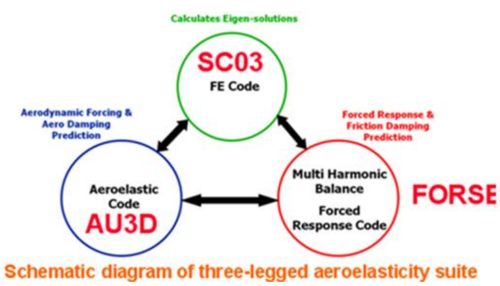

Figure 1 An in-house aeroelasticity suite [15, 16].

The CFD analyses described here are performed using the Spalart-Allmaras turbulence model [8, 9, 10, 18 and 19]. Mixing-plane boundary conditions are used in the multi-bladerow-steady-state-solution computations. While for unsteady-flow-multi-bladerow computations, sliding-plane boundary conditions are used. The unsteady aeroelasticity computations are initiated from the steady-state solutions. Flow variables are calculated in a time-accurate fashion. At each time step, the unsteady pressures are applied to the structure and the new position of the structure is computed using the available modal information (i.e. modeshape). Any number of vibration modes can be included into the analysis. But for flutter assessment, usually only one mode is included into the analysis. The CFD mesh is moved to the new position and a new set of variables is computed. At the next time step, the new unsteady pressures are applied to the blade, and the process repeats again and again, see Fig.2. Aerofoil surface mesh motion is essential for flutter computations. The unsteady aeroelastic computations are continued until a periodic solution (in frequency of oscillation) is achieved. Aerodynamic damping computations can be performed on single-blade-passage-one-bladerow, full-annulus-single-bladerow or full-annulus-multi-bladerow (embedded-row flutter analyses) models. The single-blade-passage flutter analyses compute the logdec directly.

$$\log \mathrm{dec} = 2\pi\varsigma \quad (1)$$

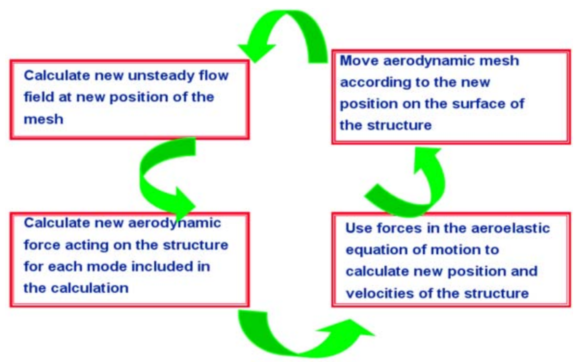

Figure 2 Fluid-structure coupling model [8, 9].

The full-annulus flutter simulations compute the ζ damping parameter. Unlike single-blade-passage flutter analyses, the full-annulus flutter method allows the computations of all nodal diameters (i.e. inter-blade-phase angles) in one single analysis run. Some AU3D flutter studies are found in references [12, 13, 14, 15 and 16].

2.2 Models and Boundary Conditions

The compressor investigated herein is an eight-stage intermediate pressure compressor comprising seventeen bladerows of stators and rotors. A single-blade-passage-one-bladerow CFD grid consists of about three hundreds thousands cells. An example of single-blade-passage grid is shown in Fig.3.

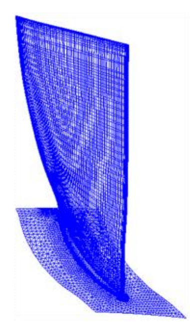

Figure 3 Single-blade-passage CFD grid.

The single-blade-passage-whole-compressor CFD mesh has approximately five millions cells. This model is illustrated in Fig.4. The unsteady flow flutter full-annulus-single-bladerow model of fifteen million cells is shown in Fig.5.

Figure 4 Single-blade-passage-compressor CFD grid.

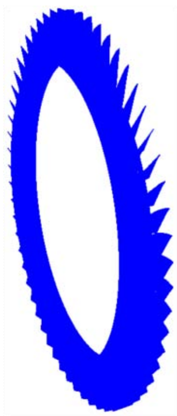

Figure 5 Full-annulus-one-bladerow mesh.

Two set of rotor running clearances are applied to the compressor and assessed for both steady-state-solution and unsteady flow computations: nominal clearances and large clearances from 1-3 times nominal clearances. In the case of large clearances, 2-3 times nominal clearances are applied to front rotors and rear rotors have clearances of about 1-2 times nominal clearances. Note that the models with large tip clearances have more grid points than those with nominal tip clearances. For the nominal tip clearances, 6-10 grid layers are used in the tip gap. While for the large clearances, the tip gap consists of about 20 grid layers. The rotor that is assessed for flutter has nominal clearances and large clearances of about 3.4 times nominal clearances. Moreover, this rotor is assessed with large parallel (i.e. parallel blade tip and casing lines) and large inclined trench clearances (i.e. inclined tip clearances).

The effects of VSV are investigated by performing steady-state-solutions with nominal VSV schedule and 5^o unganged open VSV malschedule (unganged means no proportionality between angular settings of VSVs). Note that the latter is an extreme schedule beyond normal operating conditions. The solutions from these computations are then used in unsteady flow flutter computations on the rotor of interest. The analysis speed is arbitrarily chosen for the simulations. The aerodynamic boundary conditions (BC) are also arbitrarily chosen. These are first obtained from through-flow computations. Then the inlet and exit individual BC extracted from the through-flow computations are used as initial BC conditions in AU3D steady-state-solution simulations. Note that initial aerodynamic BC from the through-flow computations can be applied to a single-bladerow or to the whole compressor model. In either case, they are applied as inlet and exit BC on single-blade-passage model or as inlet BC for the first bladerow and exit BC for the last bladerow of the whole compressor model. Note that performing flutter simulations on rotor using starting solution obtained from single-blade-passage-single-bladerow steady-state-solution analyses may yield different results from the case where the starting solution for the flutter simulations are obtained from single-blade-passage-multi-bladerow or whole compressor steady-state-solution computations. This is just to highlight the importance of the starting solutions for the unsteady flow flutter computations.

The modeshapes used in flutter simulations are obtained from FE rotor analyses. Preliminary assessment of vibration modes shows that the modeshapes obtained from FE blade alone model and FE bladed-disc model have negligible differences. Therefore, only modeshapes of FE blade alone model are used in the flutter computations. The modeshapes assessed here are first flap (flexural mode), trailing edge dominated first torsion, leading edge dominated first torsion, and second flap (flexural mode). The mode selection is based on experience that the first flap and first torsion modes are most susceptible to flutter for low values of reduced frequency parameter. These modeshapes are shown in Fig.6.

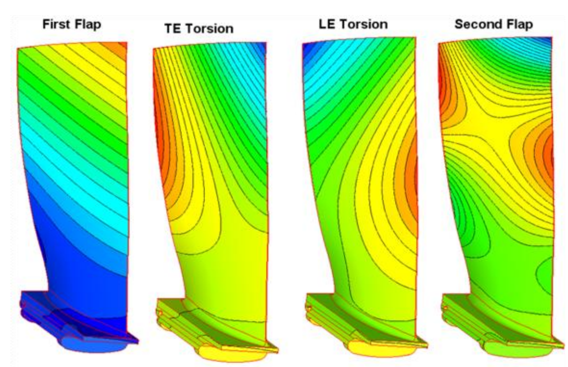

Figure 6 Vibration modeshapes (red means high and blue means low displacements) assessed for flutter.

Accuracy of computational methods and some validation of the code used herein can be found in [18, 19 and 20].

3. RESULTS AND DISCUSSIONS

3.1 Steady-State-Solution Results

As mentioned in the previous section, the steady-state-solution computations are performed on single-blade-passage-single-bladerow, single-blade-passage-stage-block and single-blade-passage-multi-bladerow (i.e. whole compressor) models. The unsteady flow flutter simulations are performed on full-annulus-single-bladerow models using the aerodynamic BC and starting solutions obtained from converged steady-state-solution computations. The study conducted herein showed that the solutions from single-blade-passage-one-bladerow and single-blade-passage-stage-block models are not appropriate (e.g. do not represent the true flow conditions of the compressor) for use as starting solutions in the unsteady flow flutter simulations. They do not represent the correct inter-stage flow interactions and conditions. This is because the original aerodynamic boundary conditions from through-flow computations do not accurately account for the flow losses. Following preliminary studies of the effects of boundary conditions on rotor flutter, it was found they differ from whole compressor steady-state-solution computations. The unsteady data presented here are all based on whole compressor steady-state flow results.

Figs.7 to 10 show plots of axial flow velocity of the whole compressor obtained from steady-state-solution computations. Fig.7 shows the axial flow velocity of the IPC with nominal tip gap at nominal VSV schedule (i.e. nominal schedule but non-optimised). In Figs.7 to 10, red means high or positive flow velocity and blue means zero or negative flow.

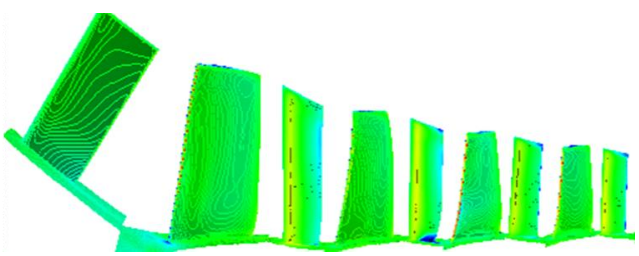

Figure 7 Nominal tip gap & non-optimised nominal schedule (Uvel).

As the VSV malschedule (i.e. unganged VSV opening) is applied to the compressor with nominal tip clearances, there is no significant changes in flow characteristics relative to nominal schedule, see Fig.8.

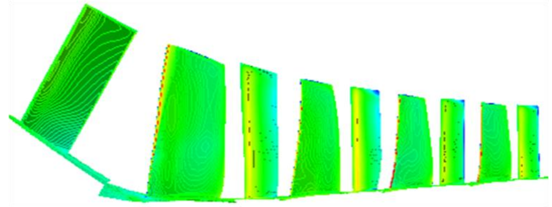

Figure 8 Nominal tip gap & VSV malschedule (Uvel).

In contrast to compressor with nominal tip clearances, relatively large tip clearances applied to the compressor cause casing-stator tip flow blockages on upstream stators for nominal VSV schedule.

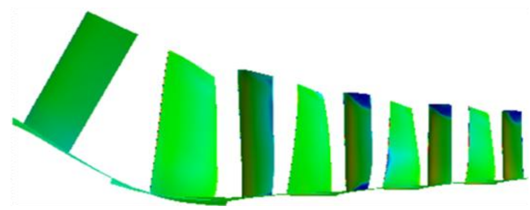

Figure 9 Large tip gap & non-optimised nominal schedule (Uvel).

The detrimental effects of large tip gap on compressor behaviour under nominal VSV operating conditions are clearly seen in Fig.9.

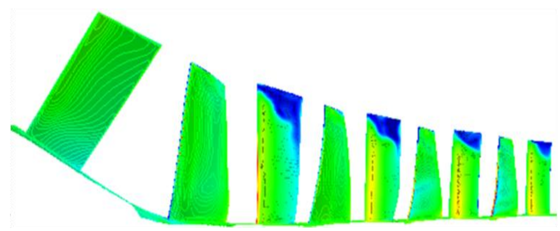

Figure 10 Large tip gap & VSV malschedule (Uvel).

The casing-stator tip flow blockage becomes more accentuated if relatively large rotor tip clearances are combined with VSV malschedule operation. As shown in Fig.10, the casing-stator tip flow losses in front stators 1 to 4 of the compressor are significant when large rotor tip clearances are combined with VSV malschedule operating conditions. The flow blockages at the tip regions can potentially lead to aerodynamic instabilities such as rotating stall and surge events.

The results described above were performed on rotors with large parallel tip clearances. Similar computations were also done on rotors with large tip clearances but that are not parallel to the casing line. A schematic diagram of inclined trench tip clearance is shown in Fig.11.

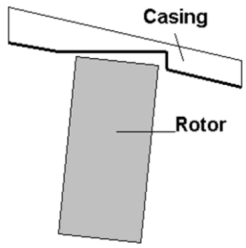

Figure 11 Schematic diagram of inclined trench tip clearance.

The steady-state-solution results from the inclined trench tip clearances (not shown here) are qualitatively similar to those of parallel tip clearances. This similarity is seen as an increase in casing-stator tip flow blockage. These results from steady-state flow computations are used in the unsteady flow flutter computations that are discussed in the next section.

3.2 Unsteady Flow Flutter Results

Additional unsteady flow computations are performed on full-annulus-multi-bladerow model with large rotor tip clearances and based on whole compressor steady-state flow results. An example of the type of model assessed is shown in Fig.12.

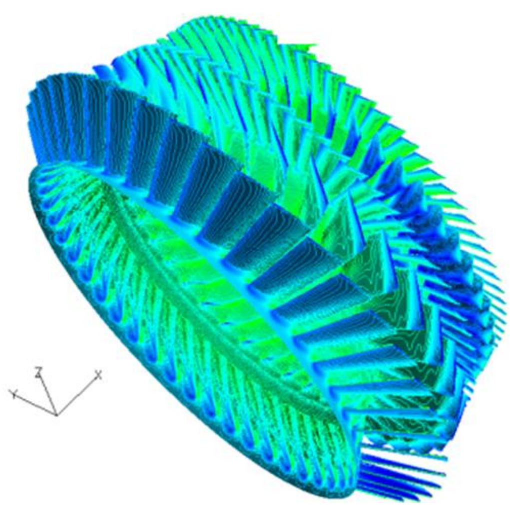

Figure 12 An illustration of a full-annulus-multi-bladerow model used in the unsteady flow simulations.

The unsteady flow simulations on the full-annulus-multi-bladerow model did not include blade motion as in flutter computations. This is just done to assess the levels of flow unsteadiness. A plot of static pressure perturbations extracted from a virtual pressure probe (e.g. numerical probe) on the casing near to the inlet of rotor of interest is shown in Fig.13. There is a slight increase in static pressure perturbations at earlier stages of computations because the mean flow from steady-state-solution computations differs slightly from the time-averaged mean flow.

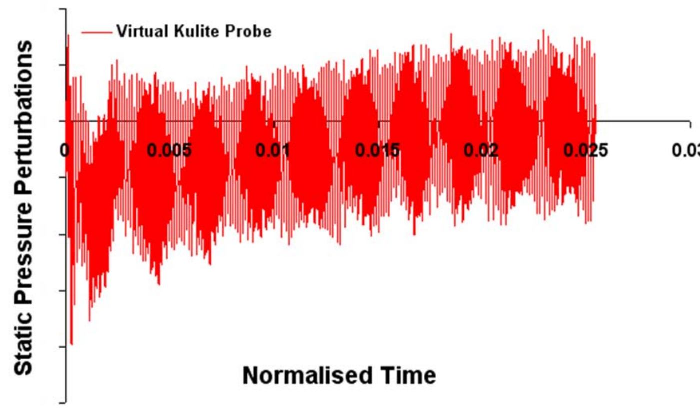

Figure 13 Static pressure perturbations from virtual pressure probe on the casing.

Using FFT techniques, the pressure perturbations in the time domain are converted to the frequency domain and then expressed in terms of engine orders (EO), which are multiples of engine shaft speed. The amplitude of static pressure perturbations versus EO plot is shown in Fig.14.

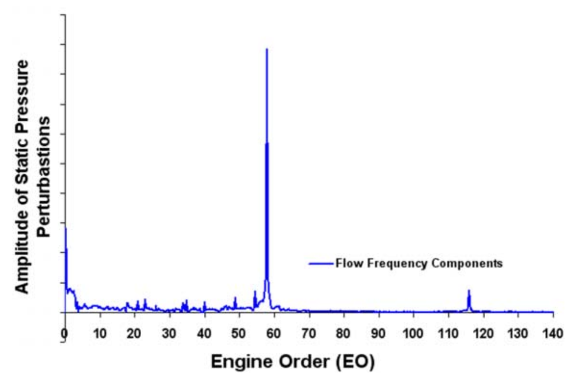

Figure 14 Amplitude of static pressure perturbations versus EO.

Fig.14 indicates the presence of integral engine order forcing resulting from upstream and downstream rotors (i.e. blade passing frequencies) and low levels of non-integral forcing. The question to whether these levels of non-integral forcing are due to the effects of tip clearance or from other sources of unsteadiness is not discussed here. This study will be the subject of future publication.

Unsteady flow flutter simulations on the full-annulus-single-bladerow models were performed for nominal tip gap, large parallel tip clearances and large inclined trench tip clearances at aerodynamic BC corresponding to non-optimised nominal VSV schedule and unganged VSV malschedule. Instantaneous plots of flow velocity perturbations on blade suction surfaces for nominal VSV schedule are shown in Fig.15. As can be seen in Fig.15, the rotor with nominal tip clearance shows little tip vortex activity close to tip leading edge. The tip flow due to vortex shedding is mainly confined to the tip trailing edge regions. In contrast, the rotors with large tip clearances, both large parallel and inclined trench tip clearances show some tip vortex flow regions close to the tip leading edge. This tip vortex characteristic appears to be more pronounced in the rotor with large inclined trench tip clearances. Away from the tip regions, in general the rotors with nominal and large tip clearances under non-optimised nominal VSV schedule operation have similar flow features.

Instantaneous plots of flow velocity perturbations on blade suction surfaces for unganged VSV malschedule operating conditions comparing rotors with nominal and large tip clearances are shown in Fig.16. Note that in Figs.15 and 16, red means high velocity perturbations and blue means low axial velocity perturbations. These instantaneous plots are just snapshots of flow velocity perturbations taken during the vibration cycles for the same contour velocity range to illustrate changes in tip vortex flow.

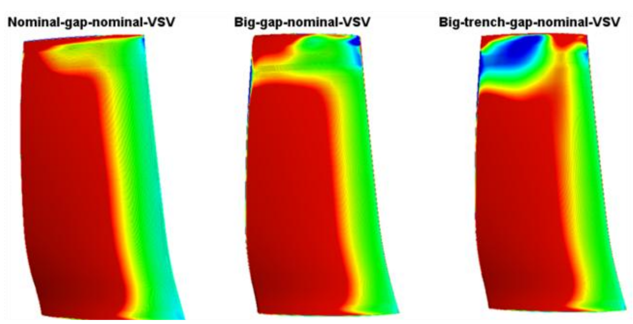

Figure 15 Nominal, big-parallel and big-trench tip clearances at nominal VSV schedule (Uvel perturbations).

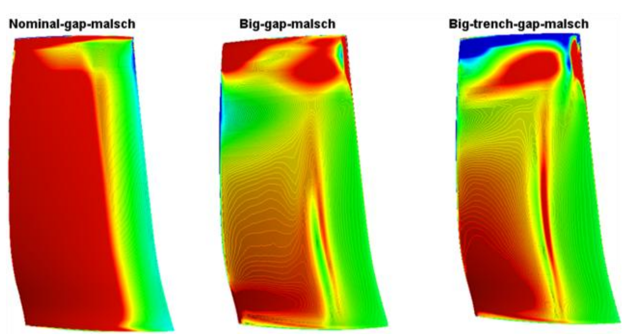

Figure 16 Nominal, big-parallel and big-trench tip clearances at VSV malschedule (Uvel perturbations).

As can be seen in Figs.15 and 16, the rotor with nominal tip clearance has very similar flow characteristics under non-optimised nominal VSV schedule and VSV malschedule conditions. However under VSV malschedule operation, more significant changes across whole suction surface are seen on rotors with large tip clearances, both parallel and inclined trench tip clearances. It is important to note that moving from nominal VSV to malschedule conditions, the tip vortex shedding effects at blade tip leading edge around 90-95% of blade span and about 20% of blade chord from LE are more visible and intense. This tip vortex activity at tip LE appears to be stronger on the rotor with large inclined trench tip clearance. The comparisons of axial flow velocity perturbations on the blade suction surface show that the rotor with nominal tip clearance is less sensitive to the effects of VSV schedule (i.e. incidence). The tip vortex activity appears to intensify on the rotors with large tip clearances and with introduction of VSV malschedule. Plots of entropy streamlines of the rotor with nominal, big-parallel and big-trench tip clearances are shown in Figs. 17, 18 and 19.

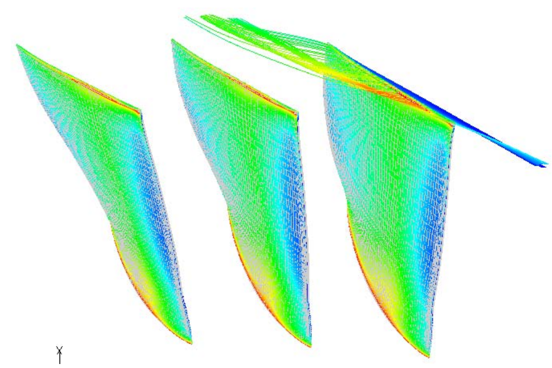

Figure 17 Tip flow entropy streamlines of the rotor with nominal clearances at VSV malschedule (red means high entropy and blue represents low entropy).

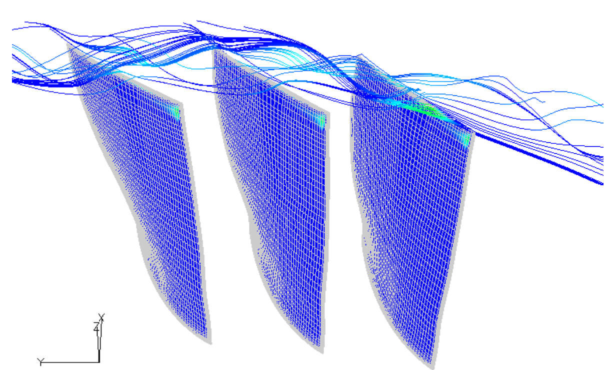

Figure 18 Tip flow entropy streamlines of the rotor with big-parallel clearances at VSV malschedule (red means high entropy and blue represents low entropy).

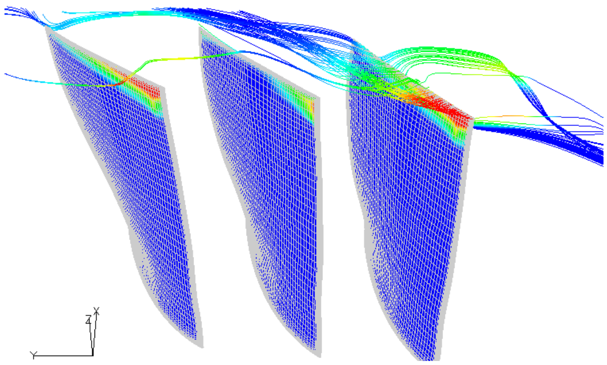

Figure 19 Tip flow entropy streamlines of the rotor with big-trench clearances at VSV malschedule (red means high entropy and blue represents low entropy).

As shown in Figs. 17 to 19, there is a very clear distinction in tip flow entropy streamlines between the rotors with nominal and large tip clearances. Reverse flow and vortex spillage over adjacent blades are seen in the rotors with large tip clearances. The rotor with big-trench clearance appears to have higher levels of entropy at the blade leading edge tip than the rotor with big-parallel clearance. The tip flow vortex spillage for the rotors with large tip clearances resembles to that described by both Kielb [3, 4] and Thomassin [7].

Flutter simulations were performed on the rotor of interest using modeshapes shown in Fig.6, first flap (flexural mode), TE dominated first torsion, LE dominated first torsion and second flap (flexural mode) respectively. Note that here only one mode was investigated in each flutter analysis (the modes described above are not assessed simultaneously although the code allows simultaneous assessment of all these vibration modes). Only the results from the least flutter stable mode (e.g. first flap mode) are presented here. The torsion modes and second flap modes are stable for both rotors with nominal and large tip clearances operating under nominal VSV schedule and VSV malschedule. The aerodynamic damping plots of the rotor with nominal tip clearance are shown in Fig.20.

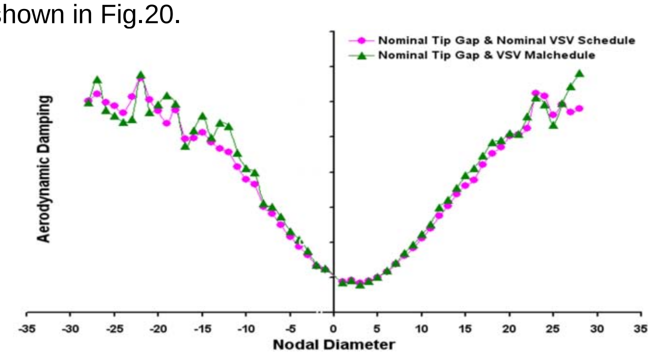

Figure 20 First flap mode aerodynamic damping characteristics of the rotor with nominal tip clearance.

As shown in Fig.20, the rotor with nominal tip clearance is flutter stable across the whole range of nodal diameters (e.g. inter-blade-phase-angle) in first flap mode for both nominal VSV schedule and VSV malschedule. Low nodal diameters close to zero are the least stable ones. The rotor does not flutter. Plots of aerodynamic characteristics of the rotors with large tip clearances are shown in Figs.21 and 22.

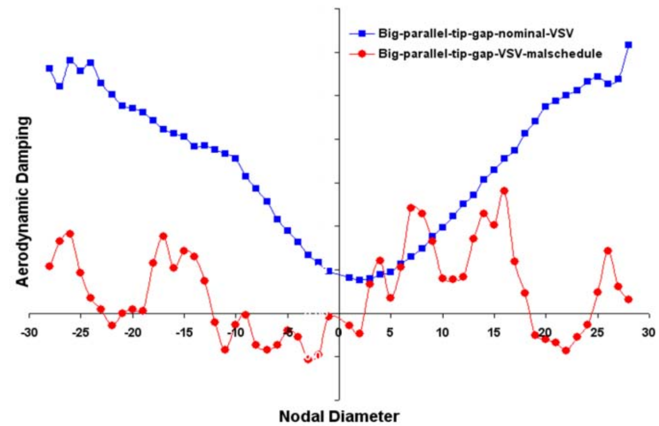

Figure 21 First flap mode aerodynamic damping characteristics of the rotor with large parallel tip clearance.

Rotors with large tip clearances, parallel and trench clearances are also flutter stable in first flap mode for nominal VSV schedule. As can be seen in Figs. 20, 21 and 22, the first flap mode aerodynamic damping characteristics of the rotors with nominal and large tip clearances are very similar and flutter stable.

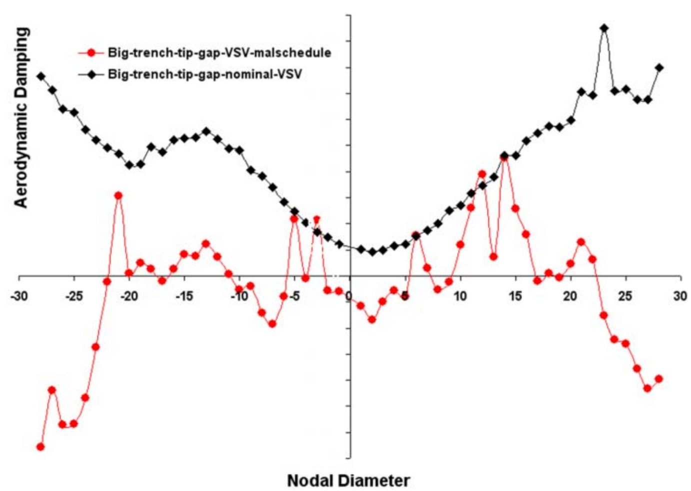

Figure 22 First flap mode aero damping characteristics of the rotor with large inclined trench tip clearance.

Both rotors with parallel and trench tip clearances fall into flutter instability over a number of nodal diameters when unganged VSV malschedule is applied. The results shown in Figs.21 and 22 indicate clearly that large tip clearances have negative effects on flutter stability of compressor rotors. These negative effects would appear to increase with increase in flow incidence resulting from the application of VSV malschedule. The mechanism that drives this kind of flutter instability is controlled by the strength and location of tip vortex shedding. The tip vortex pulsations at the blade tip LE feed more aerodynamic energy into blade that cannot be fully dissipated by material or mechanical damping if present and hence the blade falls into flutter instability (i.e. tip vortex driven flutter). In rotors with large tip clearance, small offsets in blade tip flow can trigger or prevent its occurrence.

In order to predict the tip vortex driven flutter instability, the rotor flutter simulations need to be performed using correct geometries and correct steady-state-solution aerodynamic boundary conditions obtained from whole compressor models.

4. CONCLUSIONS

Here, this paper has shown that the compressors with large rotor tip running clearances are prone to tip vortex driven flutter instability. The aerodynamic losses on the rotor with large tip clearances increase with other rotors having also large tip gaps. The flutter simulations predicted the first flap vibration mode as the least stable vibration mode for the aerodynamic boundary conditions considered here. The flutter instability predicted on the rotors with large tip clearances is driven by oscillating tip vortices on blade suction surface close to the blade tip leading edge. The flow in the rotor tip gap is mostly stalled and tip vortices oscillations are close to blade tip leading edge. The strength of these oscillating vortices appears to increase with increase in variable stator vane malschedule or negative incidence. Small changes in aerodynamic conditions can offset these instabilities. These studies indicate that the main ingredients for the occurrence of these phenomena are likely to be excessively large rotor tip running clearances combined with significant changes in flow incidence.

5. ACKNOWLEDGMENTS

The author would wish to thank Rolls-Royce plc for allowing this publication.

6. REFERENCES

[1] Huang, X., He, L. and Bell, D. L., “Effects of Tip Clearance on Aerodynamic Damping in a Linear Turbine Cascade”, Journal of Propulsion and Power, Vol.24, no.1 pp26-33, January 2008.

[2] Yang, H. and He, L., “Experimental Study on Linear Compressor Cascade with 3-D Blade Oscillation” AIAAA Journal of Propulsion and Power Vol.20, no.1, pp180-188, January-February 2004.

[3] Kielb, R., Hall, K. C., Spiker, M. and Thomas J. P., Non-synchronous Vibration of Turbomachinery Airfoils, Final Report AFORSR Contract F49620-03-1-0204 March 2006.

[4] Kielb, R., Thomas, J. P., Barter, J. W. and Hall, K. C., “Blade Excitation by Aerodynamic Instabilities -A Compressor Blade Study”, Proceedings of the ASME Turbo Expo 2003, GT-2003-38634, Atlanta, Georgia, June 2003.

[5] Mailach, R., Sauer, H. and Vogeler, K., “The Periodical Interaction of the Tip Clearance Flow in the Blade Rows of Axial Compressors”, ASME Paper no. GT-2001-0299, 46th ASME Turbo Expo, June 4-7 2001, New Orleans, Louisiana, USA.

[6] Mailach, R., Lehmann, I. And Vogeler, K., “Rotating Instabilities in an Axial Compressor Originating from Fluctuating Blade Tip Vortex”, ASME Paper no. GT-2000-0506, 45th ASME Turbo Expo, May 8-11 2000, Munich, Germany.

[7] Thomassin, J. and Vo, D. H., “Blade Tip Clearance Flow and Compressor NSV: The jet Core Feedback Theory as the Coupling Mechanism”, Proceedings of ASME Turbo Expo, Paper no. GT-2007-27286, May 14-17 2007, Montreal, Canada.

[8] Vahdati, M. and Imregun, M., “Non-linear aeroelasticity analyses using unstructured dynamic meshes”, Proc. Instn. Mech. Engrs., Part C, Journal of Mechanical Engineering Science, 1996, **210** (C6), 549-564.

[9] Sayma, A. I., Vahdati, M., Sbardella, L. and Imregun, M., “Modelling of Three-Dimensional Viscous Compressible Turbomachinery Flows Using Unstructured Hybrid Grids”, AIAA Journal, Vol.38, No.6, June 2000, 945-954.

[10] Sayma, A.I., Vahdati, M. and Imregun, M., “Multi-bladerow fan forced response predictions using an integrated three-dimensional time-domain aeroelasticity model”, Proc. Instn. Mech., Engrs., Vol.214, Part C, IMechE 2000, 1467-1483.

[11] Vahdati, M., Sayma, A.I., Lee, S.J. and Imregun, M., “Multi-bladerow Forced Response Predictions

for a Rig with Articulated Inlet Guide Vanes", In Proceedings of the National 4th High Cycle Fatigue Conference, Monterey, USA, 1999.

[12] Peng, C. and Vahdati, M., "The Effects of Fundamental Mode Shapes on Flutter Stability of an Aero Engine Compressor Blades: Introduction of a Modified Reduced Frequency Parameter", 7th National Turbine High Cycle Fatigue (HCF) Conference, 14-17 May 2002, Palm Beach Gardens, USA.

[13] Simpson, G., Peng, C., Vahdati, M., Sayma, A.I. and Imregun, M., "Influence of Rotor Blade Damage on Flutter and Forced Response of High Pressure Compressor Blades", 8th National Turbine High Cycle Fatigue (HCF) Conference, Hyatt Regency, USA, 14-16 April 2003.

[14] Peng, C. and Aurifeille, E., "The Nature of Choke Flutter in Low and High Pressure Compressors", 9th National Turbines High Cycle Fatigue (HCF), Pinehurst, 16-19 March 2004, USA.

[15] Peng, C., Zilli, A., "A Methodology to Predicting Total Damping of Axial Compressor Shrouded Stator Vanes", GT2009-60359, Proceedings of ASME Turbo Expo 2009, Orlando, Florida, USA.

[16] Peng, C. "Predictions of Damping of Single Vane and Vane Segment of Axial Core Compressors", ISUAAAT 12, Imperial College of London 1-4 September 2009.

[17] Peng, C. and Petrov, E., "Prediction of Mechanical Damping for Core Compressor Blades and Vanes", 10th National Turbine Engine High Cycle fatigue (HCF) Conference, 8-11 March 2005, New Orleans, USA.

[18] Vahdati, M., Simpson, G. and Imregun, M., "Aeroelastic Behaviour of Aero-engine Core Compressors during Rotating Stall and Surge", Proceedings of ASME Turbo Expo 2006, May 8-11, 2006, Barcelona, Spain, ASME Paper GT2006-90308.

[19] Choi, M., Vahdati, M. and Imregun, M., "Effects of Fan Speed on Rotating Stall Inception and Recovery", Proceedings of ASME Turbo Expo 2010, June 14-18, 2010 Glasgow, UK.

[20] Johann, E., Mück, B. and Nipkau, J., "Experimental and Numerical Flutter Investigation of the 1st Stage Rotor in 4-Stage High Speed Compressor", Proceedings of ASME Turbo Expo 2008, June 9-13, 2008, Berlin, Germany, ASME paper GT2008-50698.